

## Geomorphological deformation examples induced by the February 06, 2023, Pazarcık earthquake (Kahramanmaraş, Türkiye)

### 06 Şubat 2023, Pazarcık (Kahramanmaraş, Türkiye) depreminin neden olduğu jeomorfolojik deformasyon örnekleri

Hüseyin Turoğlu<sup>a</sup>  Osman Sarıgül<sup>b</sup> 

<sup>a</sup> İstanbul University, Faculty of Letters, Department of Geography, İstanbul, Türkiye.

<sup>b</sup> İstanbul University, Institute of Social Sciences, Geography Doctorate Program, İstanbul, Türkiye,

ORCID: H.T. 0000-0003-0173-6995; O.S. 0000-0002-4677-5157

#### BİLGİ / INFO

Geliş/Received: 12.06.2023

Kabul/Accepted: 10.07.2023

#### Anahtar Kelimeler:

06 Şubat 2023 Depremi

Pazarcık Fayı

Sol yanal atım

Jeomorfolojik

Deformasyon

#### Keywords:

February 06, 2023

Earthquake

Pazarcık Fault

left lateral offset

Geomorphological

Deformation.

#### \*Sorumlu yazar/Corresponding author:

(H. Turoğlu) [turogluh@istanbul.edu.tr](mailto:turogluh@istanbul.edu.tr)

DOI: 10.17211/tcd.1313551



#### Atıf/Citation:

Turoğlu, H., & Sangül, O. (2023). Geomorphological deformation examples induced by the February 06, 2023, Pazarcık earthquake (Kahramanmaraş, Türkiye). *Türk Coğrafya Dergisi*, (83), 23-34.  
<https://doi.org/10.17211/tcd.1313551>

#### ABSTRACT / ÖZ

The left-laterally strike-slip Pazarcık fault is one of the East Anatolian Fault Zone (EAFZ) segments. On February 6, 2023, the ±85 km long Pazarcık fault generated a highly destructive Mw=7.7 earthquake. This study aims to explain the geomorphological deformations caused by the February 6, 2023, Pazarcık earthquake with typical examples. The surface rupture of the earthquake between Türkoğlu and Gölbaşı was followed precisely, and the changes in the earth's surface due to the left lateral strike-slip were determined, measured, and recorded. A DJI Phantom 4 and a DJI Mini Drone were used for aerial measurements and recordings during the fieldwork. Garmin e-Trex 10 handheld GPS and tape measure were used for terrestrial measurements.

During the field studies, the surface rupture of the earthquake was investigated from a geomorphological perspective and mapped by taking location data. It was determined by the measurements that the left lateral offset distances in the surface fracture vary between 4.0-6.5m. One of the geomorphological deformations of the February 6, 2023 earthquake is transpressional ridges and/or transtensional depressions. Transpressional shortening and/or transtensional extension deformations due to a single surface rupture are the natural consequences of the curvilinear slip plane of the left-laterally strike-slip Pazarcık fault. Liquefaction samples with different characteristics were observed in the Sakarkaya alluvial fill area within the Gölbaşı depression. Rockfalls occurred on sandstone, mudstone, and limestone rock slopes weakened by the discontinuity due to the density of cracks outcropping in the valley where the surface rupture passes in the Kartal, Sakarkaya section. During field studies, slides and spreading were also observed. Typical examples of slide occurred on the unconsolidated fill ground on the south coast of Gölbaşı Lake with a slight slope towards the lake as a result of the vibration effect of the earthquake. In addition, the vibration effect of the earthquake caused lateral spreading deformations in the artificial fillings of road and road junction structures.

*Sol yanal atımlı Pazarcık fayı; Doğu Anadolu Fay Zonu (DAFZ) nun segmentlerinden biridir. ±85 km uzunluğundaki Pazarcık fayı 06 Şubat 2023 tarihinde Mw=7.7 büyüklüğünde bir deprem üretmiştir. Bu çalışmada, 06 Şubat 2023 Pazarcık depreminin neden olduğu jeomorfolojik deformasyonların, tipik örneklemeler ile açıklanması amaçlanmıştır. Depremin, Türkoğlu-Gölbaşı arasındaki yüzey kırığı birebir takip edilerek, sol yanal atım nedeniyle yeryüzünde meydana gelen değişimler tespit edilmiş, ölçümlenmiş ve kayıt edilmiştir. Saha çalışması sırasında havadan yapılan ölçüm ve kayıtlarda DJI Phantom 4 ve DJI Mini Drone kullanılmıştır. Yersel ölçümlerde ise Garmin el GPS ve şerit metre kullanılmıştır.*

*Arazi çalışmaları sırasında depremin yüzey kırığı jeomorfolojik perspektifte araştırılmış, lokasyon verisi alınarak, haritalanmıştır. Yüzey kırığındaki sol yanal atım mesafeleri 4-6.5m arasında değişiklik gösterdiği yapılan ölçümlerle tespit edilmiştir. 06 Şubat 2023 depreminin jeomorfolojik deformasyonlarından biri sıkışma sırtları ve açılma çöküntüleridir. Bu morfolojik deformasyonlar; sol yanal atımlı Pazarcık fayının eğrisel kayma düzleminin ortaya çıkardığı doğal sonuçlardır. Farklı özelliklere sahip sıvılaşma örnekleri Gölbaşı depresyonunun Sakarkaya mevki alüvyial dolgu sahasında gözlenmiştir. Kaya düşmeleri Kartal-Sakarkaya bölümünde yüzey kırığının içinden geçtiği vadide yüzeylenen çatlak yoğunluğu nedeniyle süreksizliğin zayıflatığı kumtaşı, çamurtaşı, kireçtaşı yamaçlarında meydana gelmiştir. Saha çalışmaları sırasında kayma ve yayılmalar da gözlenmiştir. Kaymaların tipik örnekleri Gölbaşı Gölü'nün güney kıyısında göle doğru az eğimli konsolide olmamış dolgu zeminde depremin vibrasyon etkisi ile meydana gelmiştir. Yine depremin vibrasyon etkisi yol ve kavşak inşaatlarına ait yapay dolgulara yanal yayılma deformasyonlarına neden olmuştur.*

## 1. Introduction

Two major earthquakes occurred in Kahramanmaraş (Türkiye) on February 06, 2023. One is the Pazarcık (Kahramanmaraş) (37.236 N – 37.057 E) earthquake with a magnitude of  $M_w=7.7$ , which occurred at 04:17 local time. The other is the earthquake whose epicenter was Elbistan (Kahramanmaraş) (38.089 N – 37.239 E) at 13:24 local time on the same day, and its magnitude was recorded as  $M_w=7.6$  (Figure 1). Also, two

major earthquakes occurred on February 06, 2023; at 04:26 local time, the epicenter was Nurdağı (Gaziantep) with  $M_w=6.4$ , and at 04:36 local time, the epicenter was İslahiye (Gaziantep) with  $M_w=6.5$ . Then on February 20, 2023, at 20:04 local time, the epicenter was Defne (Hatay), where  $M_w=6.4$  were recorded. Between February 06, 2023, and May 07, 2023, a total of 560 earthquakes with  $M \geq 4.0$  occurred (AFAD, 2023; BDTİM, 2023; KRDAE, 2023; Kürçer et al., 2023a; Kürçer et al., 2023b, Utkucu et al., 2023).

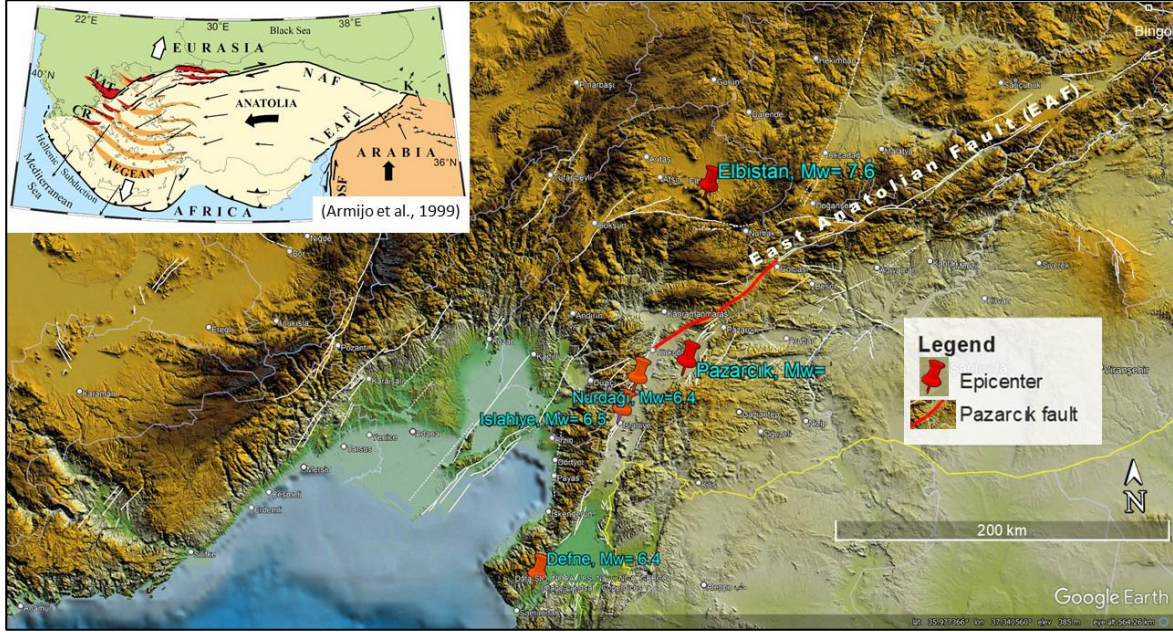


**Figure 1:** Anatolian plate and main tectonic lines (in small frame) (Armijo et al., 1999), East Anatolian Fault (EAF) (MTA, 2023 ve ATAG, 2023), Pazarcık segment (red line) (Karabacak et al., 2023), locations of February 06, 2023, and February 20, 2023 earthquakes (AFAD, 2023; Kürçer et al., 2023b; Utkucu et al., 2023).

## 2. Material and Method

Due to the consequences of the earthquakes, 11 provinces were declared as disaster zones. According to official records, more than 50,000 people lost their lives due to the earthquakes, more than half a million buildings were damaged, communication, transportation, and energy infrastructure were damaged in the earthquake zone, and significant financial losses occurred (SBB, 2023). Tectonic movements that caused the earthquakes also caused morphological changes on the earth's surface. In this research, the geomorphological deformations due to the tectonic movements that caused by the Pazarcık earthquake of February 06, 2023 were investigated, and typical representative geomorphic deformation examples were discussed.

The research was carried out in two stages, first as field research and then as the evaluation of field data. During the field study, the surface rupture of the Pazarcık segment was followed, and the geomorphological changes caused by the left-lateral displacement of the blocks were measured. A DJI Phantom 4 Drone, a DJI Mini Drone, Garmin e-Trex 10 handheld GPS, tape measure, and Nikon D7200 Digital camera were used in the measurements. The digital data obtained from the field studies were analyzed and mapped using Geographic Information Systems (GIS) technologies and ArcMap 10.7 software. In addition, 1/25000 scale topography and geological maps of the study area, SRTM, and ATLAS Applications were also used.

## 3. Results

### 3.1. Tectonic and Geomorphic Setting

The compressive stress due to the northward movement of the Arabian plate caused the Anatolian block to shift westwards through the North Anatolian Fault (NAF) and the East Anatolian Fault (EAF) (Şengor & Yılmaz, 1981; Dewey et al., 1986; Hempton, 1987; Yılmaz, 1993; Armijo et al., 1999) (Figure 1). The EAF, which is one of the two main strike-slip faults, is an active left-lateral strike-slip fault zone with a length of approximately 550 km, running roughly from Samandağ (Hatay) in the south to Karlıova (Bingöl) in the north (Figure 1). The section of the DAF between Türkoğlu and Gölbaşı is referred to as the Pazarcık segment (Khalifa et al., 2018; Güvercin et al., 2022; Karabacak et al., 2023; Kürçer et al., 2023a; Kürçer et al., 2023b) (Figure 2).

The Pazarcık segment is represented by a curvilinear surface rupture running roughly northeast-southwest between Türkoğlu and Gölbaşı (Figure 2). The southern part of the surface rupture continues, passing through the alluvial plain of the Türkoğlu depression, including the Türkoğlu and Kılılı settlements, and then turning slightly to the east-northeast within the Kuyumcular, Tevekkeli, and Çiğli hillside settlements. These slopes are generally represented by ophiolitic melange. The ophiolitic melange series has a limited distribution in the NE direction. In the ENE direction are sandstone, mudstone, and limestone outcrops around Kartal and Sakarkaya. The surface rupture of the left lateral strike-slip fault is traced in the northeast direction from Çiğli within this lithologically diverse high mass (Figure 2).

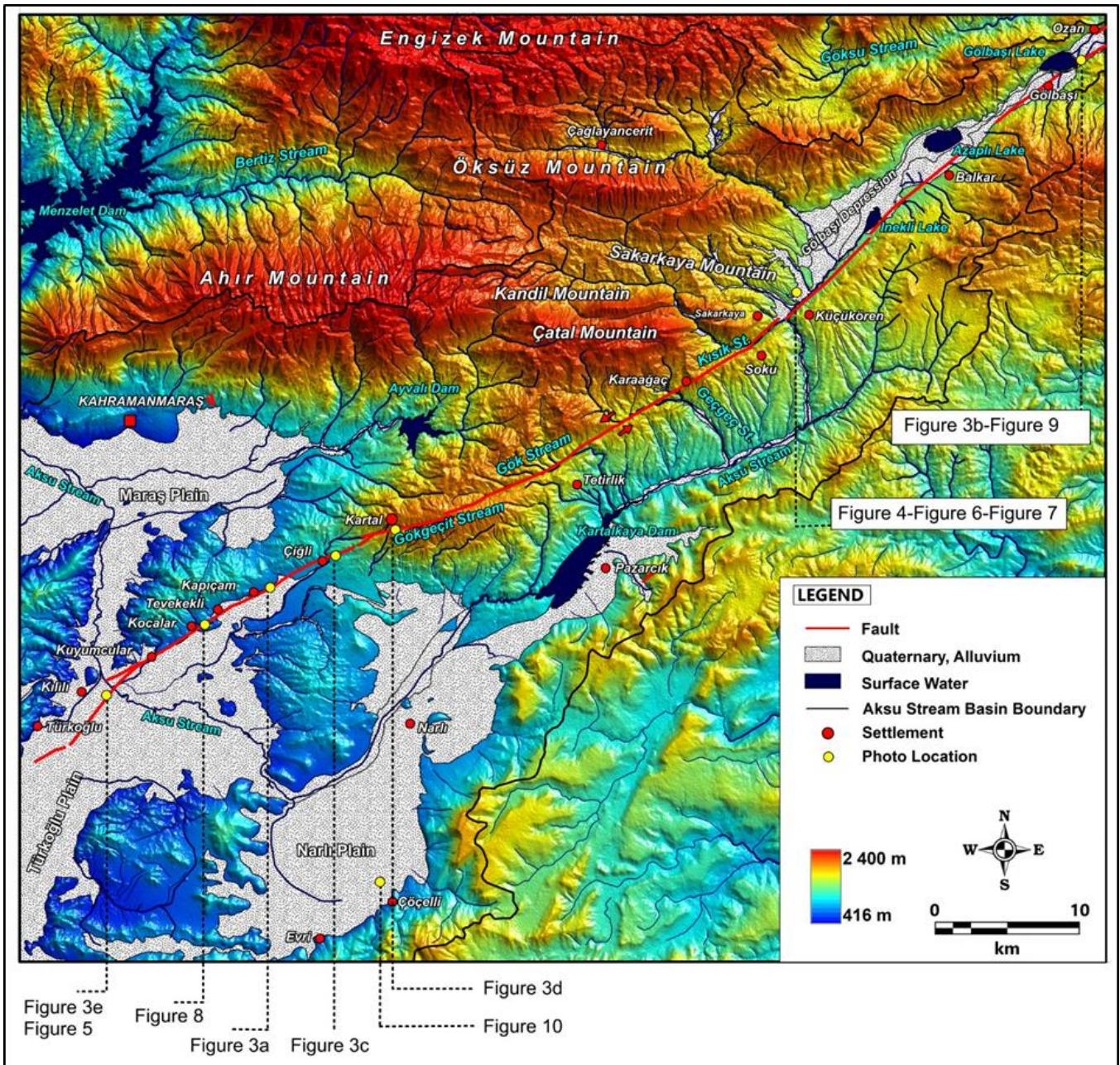


Figure 2: EAF Pazarlık segment and locations of described geomorphological deformation samples of the tectonic movement.

The Çiğli, Kartal, and Sakarkaya section of the Pazarlık segment between 900-1200 m elevations is located in a rugged morphology, and the surface rupture of the fault is oriented roughly northeast-west-southwest in this section (Figure 2). Then, the surface fracture of the left laterally thrust fault is traced in the northeast-southwest direction in the Gölbaşı depression. The Gölbaşı depression is an alluvial-filled tectonic plain between Sakarkaya and Gölbaşı and is largely occupied by the Inekli, Azaplı, and Gölbaşı lakes and their shoreline reeds and marshes (Figure 2). The strike-slip fault deformation effect of the DAF Pazarlık segment has also significantly affected the drainage system. Kısık Stream, Geçgeç Stream, Killisu (Gök) Stream and some small streams are tributaries joining from the north to the Aksu Stream, and these streams offset about 1000 m towards the southwest (left) on the Pazarlık fault at the Çiğli and Sakarkaya section. The offset on streams between Çiğli and Sakarkaya reflects the deformation of the tectonic movement on the drainage system (Figure 2) (Turoğlu & Sarıgül, 2023).

### 3. 2. Geomorphic deformations

The geometry of the surface rupture, transpressional ridges, transtensional depressions, liquefaction structures, offsets on natural and artificial structures, and slope failers (rock falls, slides) are the major geomorphological deformation types caused by moving blocks during the DAF Pazarlık earthquakes on 06 February 2023. These geomorphological deformation types are discussed here, with an example to introduce their characteristics (Figures 1 and 2).

#### 3.2.1. Surface rupture and seismic displacement

Although its main direction is SW-NE, the  $\pm 85$  km long left-lateral strike-slip fault shows a loose sinusoidal curvature (Figure 2). While the surface rupture of the left lateral strike-slip fault is roughly in the SW-NE direction between Türkoğlu and Çiğli, it makes a slight turn towards ENE in the Çiğli-Kartal section and continues roughly in the WSW-ENE direction. The surface fracture then turns NE in the vicinity of Sakarkaya slightly and is followed in this direction in the Gölbaşı depression. The strike of the fault in Gölbaşı depression is

roughly SW-NE. Large and small-scale curvatures of the fault caused morphological deformations such as a transtensional extension by releasing a bend in the alluvial plain in the NE Türkoğlu section, and a transpressional ridge by restraining the bend in the alluvial plain in the NE Sakarkaya section. The offset distances on the Pazarcık fault are unequal throughout the surface rupture, and offsets between 4.0-6.30 m were

measured. However, the typical offset distance is approximately 5m.

Measurable displacement deformations in natural and artificial structures with distinct boundary features, such as roads, natural drainage channels, water channels, land boundaries, and railways, were considered the defining evidence of the sinistral strike-slip fault (Figure 3).

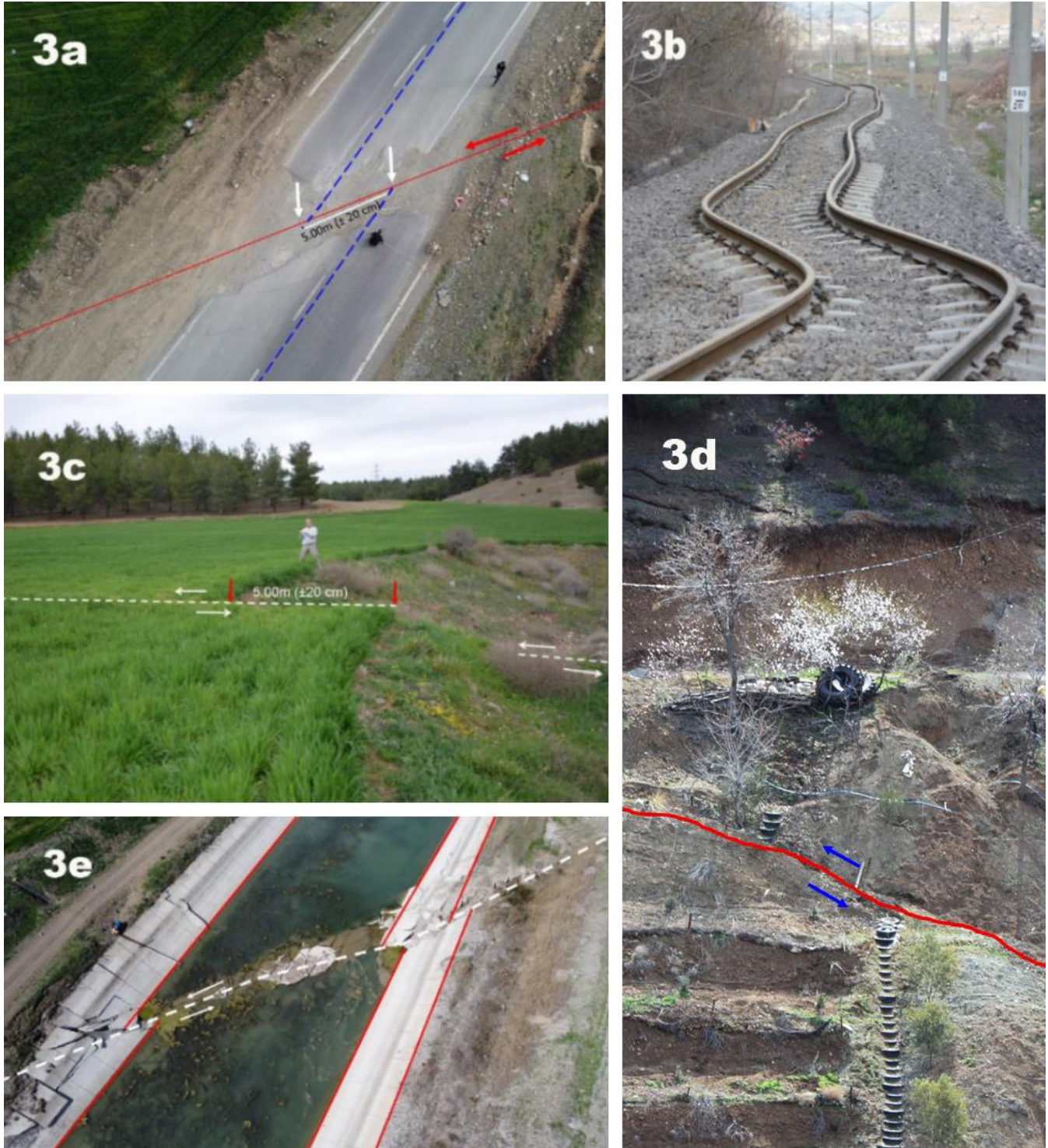


**Figure 3:** Evidence of offset that occurred on the sinistral strike-slip Pazarcık fault with the February 06, 2023 earthquake (3a: The offset on Gaziantep-Kahramanmaraş highway, 3b: Gölbaşı town, 3c: East of Çiğli village, 3d: Kartal village, 3e: Southeast of Kılılı) (Figure 2).

### 3.2.2. Transpressional ridges and transtensional depressions

In the strike-slip fault mechanism, the horizontally and oppositely displaced blocks cause surface deformation such as the uplifts by compression and subsidence by extension

during these movements. These surface deformations come from single restraining and releasing bends, or stepovers due to the curvature of the strike-slip fault line (McClay & Bonora,

2001; Cunningham & Mann, 2007). In strike-slip faults, the restraining bends or stepovers create the effect of Transpressional shortening and Transtensional extension zones. Transpressional shortening causes local linear ridges on the topography surface that continue along the surface fracture. They represent the anticlinal uplifts in a typically positive flower structure. Transtensional extension creates depression deformation (Christie-Blick & Biddle, 1985; Dewey et al., 1986; Sylvester, 1988; McClay & Bonora, 2001; Burbank & Anderson, 2008; Huang & Liu, 2017). The depressions formed by single releasing bends or stepovers create oblique displacements with vertical displacement components (Christie-Blick & Biddle, 1985; Cunningham & Mann, 2007). Due to strike-slip faults, the changes in the topography surface differ depending on whether the ground is sedimentary or rocky and its resistance against the deformation, as well as the magnitude of compressional and tensional forces. The compression and opening structures formed on the surface rupture of the Pazarcık segment, which forms part of the EAF zone (Figure 1), are due to the curvilinear character of the Pazarcık fault (Figure 2) (Turoğlu & Sarigül, 2023).

### 3.2.2.1. Transpression structure

After 06 February 2023, earthquake-induced compression

ridges (linear uplifting heave structures) were observed on the flat and almost flat, young alluvial accumulation morphologies in the Sakarkaya region of the surface rupture between Sakarkaya and Gölbaşı (Figure 3). These deformation structures are reliefs in a fan cross-section shape rising from the surface and continuing along the surface rupture of the fault. Although dimensions vary, heights between 0.70-1.50 m and widths between 3.50-7.00 m were measured in the field. The ridge surface is characterized by longitudinal cracks forming stepping, with elevation differences (Figure 4) (Turoğlu & Sarigül, 2023). The ridge's fractured and irregular surface structure is within the boundary of the fan-shaped relief surface. These morphologies are also described as classical, positive flower structures (Huang & Liu, 2017). The compression structures forming a linear ridge were formed where the parabolic curve in the surface fracture was restricted or prevented to the left. The relationship between the inhibition of the left offset and the compressive stress determined the rise and ridge formation dimensions. This is because, while the compression structure did not develop within the eastern part of the Gölbaşı depression, the compression ridge starts to form within the western part of the Gölbaşı depression, in the alluvial plains near Sakarkaya. The dimensions of the compression ridges continue to increase in the direction of Mount Sakarkaya.

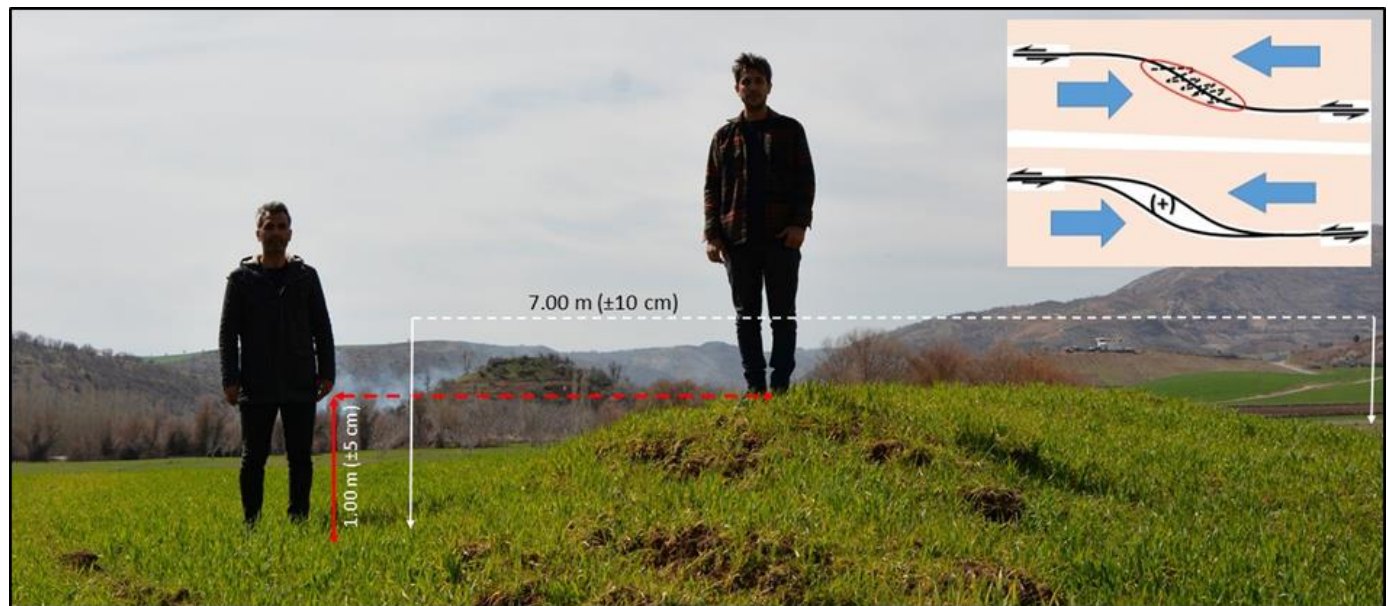


**Figure 4:** Dimensions of the transpression zones (height, width, length) were formed under the control of the compression process (Figure 2). Depending on the compaction pressure, the deformation dimensions change.

### 3.2.2.2. Transtension structure

The February 06, 2023 earthquake caused local subsidence on the surface rupture of the sinistral strike-slip Pazarcık fault. These depressions were formed by the blocks moving in the opposite direction, in parabolic linearity, moving away from each other. The asymmetric depression (Figure 5) formed on the SW part of the Pazarcık fault near Türkoğlu represents this type of transtensional depression. The sinistral strike-slip in the region is in SW-NE directions. Depths of 1.00-1.70 m were measured along the SE boundary and 0.50-1.00 m along the NW boundary of the depression shown in Figure 5. In the NW bloc bounding the depression, the vertical displacement varies between 0.0-1.0 m. The releasing bend depression reaches a width of  $\pm 30.00$  m

(Figure 4), and the surface ruptures approach each other in the direction of Türkoğlu (Figure 5).

The releasing bend depressions on the Pazarcık fault also contain oblique displacements. Oblique displacement in a depression (Figure 5) was measured up to  $\pm 1.7$  m during field studies. The local ponding developed on the deeper SW surface fracture side of the depression (Figure 5) is one of the largest ponds on the surface rupture. But in most cases, the morphological deformations that occur with vertical and horizontal displacements of a few meters on these accumulation plains, and agricultural areas are rapidly erased from the topography surface by the interventions of farmers with tractors.

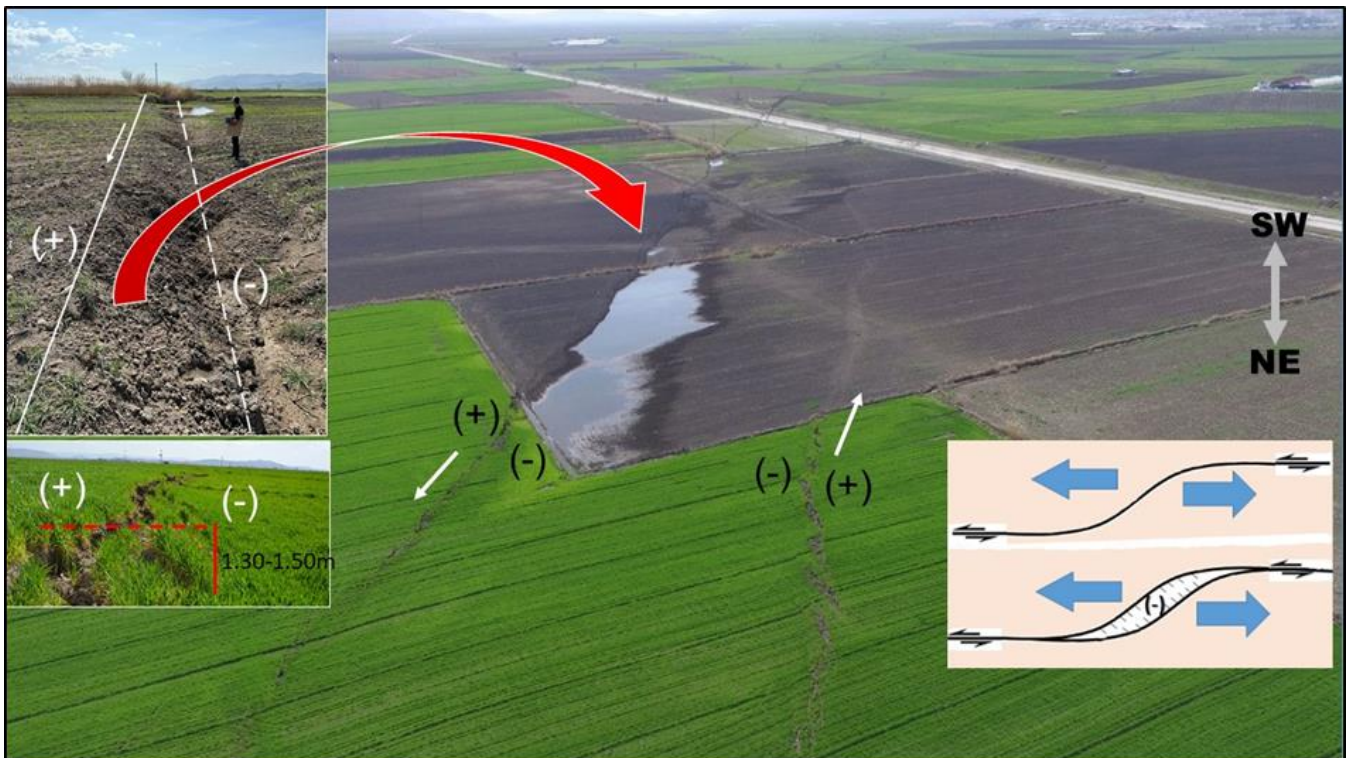


**Figure 5:** This depression near Türkoğlu is one of the depressions caused by blocks moving away from each other on the curvilinear left-lateral strike-slip fault (Figure 2).

### 3. 2. 3. Liquefaction structures

In water-saturated, fine-grained dendritic alluvial-filled ground, the tensile-compressive stress effect caused by the earthquake creates a pore water pressure in the soil, and liquefaction occurs. As the pore water pressure increases, the contact between the grains decreases, the water concentration increases, and this unit shows fluid behavior. In compression structures on strike-slip faults, compressive stress causes this fine-grained fluid to rise to the surface, and liquefaction cone structures and liquefaction cracks and depressions may develop (Figure 6) (NRC, 1985; Vallejo, 1992; Rauch, 1997; Sciarra et al., 2012; Tuttle et al., 2019; Shao et al., 2020).

The Sakarkaya-Gölbaşı section of the Pazarcık fault passes through a water-saturated, young, detrital, alluvial accumulation plain belonging to Quaternary lake/marsh and river deposits (Figure 2). Typical liquefaction structures formed by the February 06, 2023 earthquake were observed along the compression ridge within the Quaternary Sakarkaya alluvial plain. Liquefaction structures have developed individually (Figure 6a) or several together (Figure 6c), or several clustered together (Figure 6d). Another liquefaction morphology observed in this region is liquefaction fissure. The

surfacing of the fluid containing fine-grained elements such as clay, silt, and sand due to liquefaction occurred in such a way to form a linear fissure (Figure 6e) (Turoğlu & Sarigül, 2023).

The liquefaction structures observed in the Sakarkaya-Gölbaşı section of the Pazarcık fault are a natural result of restraining bends stress in the curvilinear surface fracture of the fault. The compressive stress causes fine sand and silt fluid to rise through the alluvial ground to the surface and spread out in blowing. Single liquefaction cones are 50-150 cm in diameter, with cone edge heights of 20-50 cm (Figure 6a). Multiple combined liquefaction cone forms and sizes vary according to the number of fluid stacks and sand accumulation volumes (Figure 6). The liquefaction structures within the Sakarkaya alluvial plain are remarkable for their alignment in the same direction with surface rupture and compaction structures in the form of ridges. Despite removing water in the fluid after the surfacing of fluid, the clay and silt it contains accumulated at the mouth of the fine sand cone or along the fissure (Figure 6). Liquefaction sludge bubbles, liquefaction sludge flow and ponding, and liquefaction sludge blankets are other examples of liquefaction morphologies observed on or near the surface fracture after the earthquake (Figure 7).

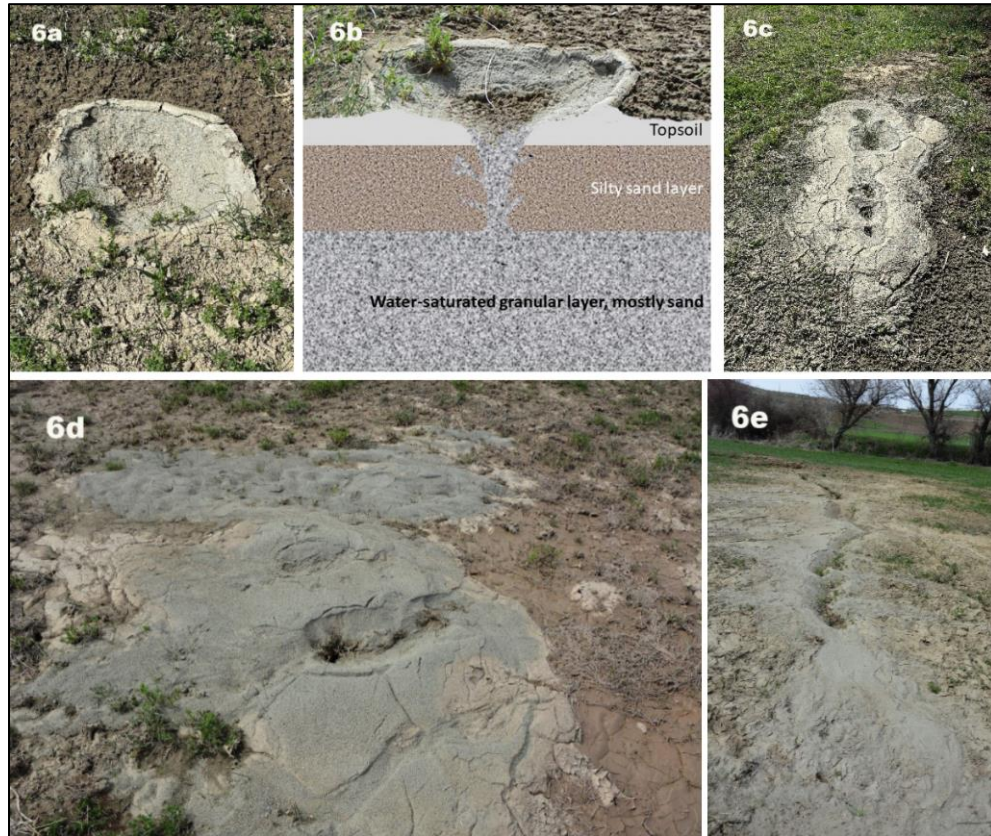


**Figure 6:** Examples of liquefaction structures. (a) Fine sand and silt blow, (b) Cross-sectional properties of a sand and silt blow, (c) Multiple grains of sand and silt blow arrays, (d) A cluster of multiple sand blows, (e) Sand and silt blow fissures (Figure 2).

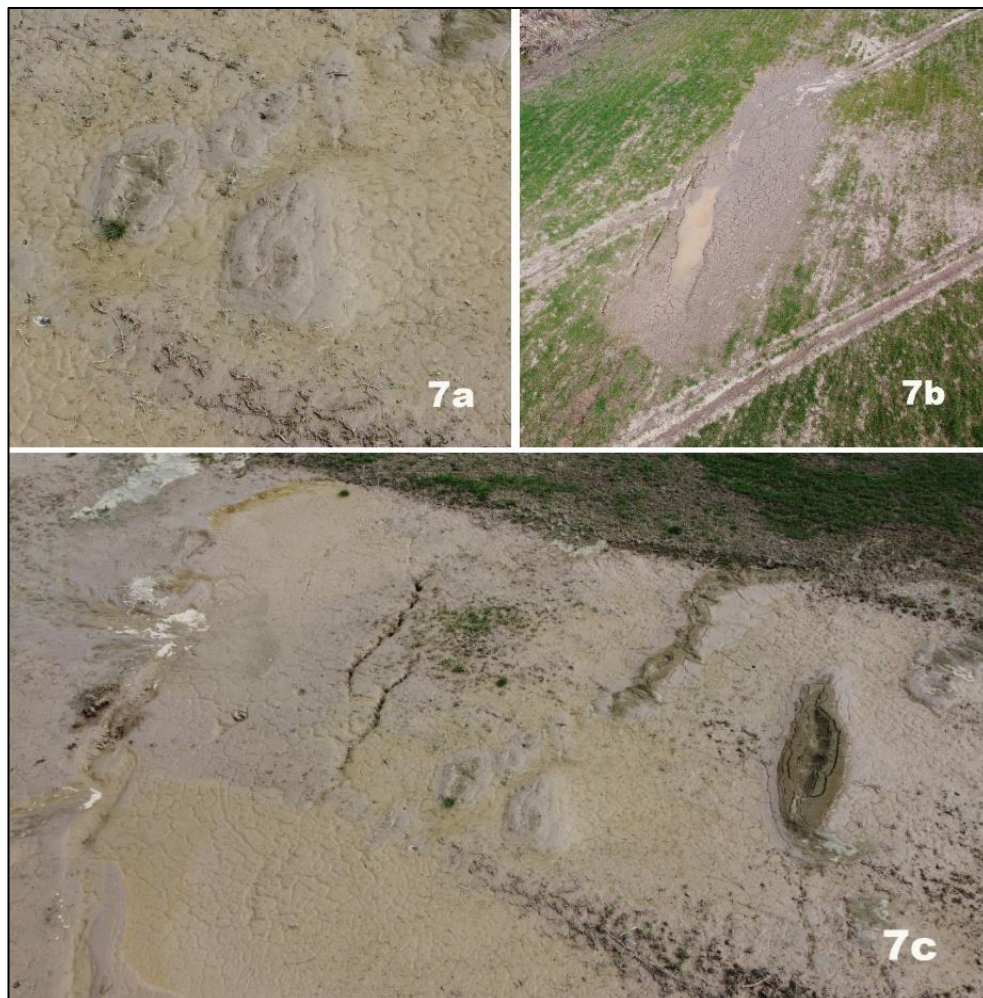


**Figure 7:** (a) Liquefaction sludge bubbles, (b) liquefaction mud flows and ponding, and (c) liquefaction sludge blankets (Figure 2).

### 3.2.4. Slope failures

Tectonic displacements along a fracture in the earth's crust cause discontinuity problems in rocks (Eitzenberger, 2012; Roy & Sarkar, 2015) and mass movements (Hack et al., 2007; Moore et al., 2012; Aydan, 2016; Tang et al., 2021; Singeisen et al., 2022) due to the stress and vibration effect of the earthquake on the rocks. Rockfalls, landslides, and slides are the most common types of slope failures on the Pazarcık segment during the February 06, 2023, Pazarcık earthquakes. Considering the morphological characteristics of earthquake-induced slope failures, it is seen that they are different from gravitation-induced slope failures. The main difference arises from the stress and vibration effect created on the ground by the tectonic movement, which is the triggering force. The common features of the slope instabilities observed in the field are related to their distribution. Slope problems were observed not only along the surface rupture of the earthquake but also on distant slopes.

#### 3.2.4.1. Rockfalls

Rockfalls triggered by tectonic movement are common on slopes where discontinuity density is high and physical weathering processes are active. The severity of discontinuity and weathering in rocks weakens or eliminates their resistance to tectonic stress-strain and vibration. In this case,

earthquake-induced rockfalls are inevitable (Moore et al., 2012; Aydan, 2016; Tang et al., 2021; Massey et al., 2022; Singeisen et al., 2022; Zheng et al., 2022). Examples of rockfalls occurred on the slopes along the surface rupture in the roughly WSW-ENE trending pressure ridge high mass between Kartal and Sakarkaya (Figure 2). The sandstone, mudstone, and especially limestone outcrops in the Sakarkaya section of the high mass consist of rocks with intense discontinuities. These discontinuities can be traced by cracks and fissures on rock surfaces devoid of soil and vegetation (Figure 8). Previous tectonic activities were primarily effective in forming and intensifying cracks and fissures in the rocks. Compression, shortening, and uplift deformation due to the curvilinearity of the left lateral strike fault is the leading cause of discontinuities in the rocks of Çataldağ, Mount Sakarkaya. It is also recognized that physical weathering processes such as freeze-thaw cycles and daily and seasonal temperature changes play an essential role in developing these cracks and fissures. The fracture and fissure systems were formed and developed by previous earthquakes on the slopes of Çataldağ and Mount Sakarkaya have prepared favorable conditions for forming rock blocks, and rock falls. The February 06, 2023 earthquakes played a triggering role in the fall of these rocks. Earthquake-induced falling blocks range from 1.00 m to several meters (Figure 8) (Turoğlu & Sarigül, 2023).



**Figure 8:** Kuyumcular-Kapıçam motorway, the surface rupture of February 06, 2023, Pazarcık earthquake crossing the left slope, causing large limestone blocks to break off and fall from this slope (Figure 2).

#### 3.2.4.2. Ground sliding and lateral spreading

Tectonic movements also play a triggering role in ground deformations in the form of sliding and spreading with the stress-strain and vibration effects they cause. Textural and structural features of the filled/covered ground, intergranular cohesion, topographic slope values, and the degree of water saturation are the determining parameters for earthquake-induced slides and lateral spreading. Ground slides do not have the general characteristic of being distributed close to the surface rupture like rock falls (Chen et al., 2018; Singeisen et al., 2022). The ground deformations such as sliding, cleavage, sinking, and collapse occurring on the shores of Gölbaşı Lake,

roughly parallel to the lake shore, are morphological deterioration and changes caused by the shaking effect of the February 06, 2023 earthquake. Examples of this type of geomorphologic deformation developed on the northern block of the surface fracture of the fault on the shores of Gölbaşı Lake (Figure 9) (Turoğlu & Sarigül, 2023). Deformation is widespread on the southern shores of Gölbaşı Lake, on a very young, unconsolidated accumulation plain sloping 2-10° towards the lake. On the lake shores where the slope is between 7-10°, the lakeward sliding, cleavages are deeper (1-1.5 m) and wider (0.5-1.5 m), and the lakeward displacements

are pronounced (Figure 9a). Where the degree of slope decreases (for shores between 2-5°), these dimensions are

also reduced, and the number of linear deformations increases, while the continuities become shorter (Figure 9b, 9c).



Figure 9: Lateral spreading on the shore of Gölbaşı Lake induced by the earthquake ground shaking (Figure 2).

The purpose of a road embankment is to raise the road platform, and this is made by compacting unconsolidated granular materials in general. The shaking force of an earthquake, however, easily weakens the cohesion between the grains in such embankment structures, destabilizing the stability of the embankment and causing cleavages, lateral spreading, and sinking deformations. In the February 06, 2023 earthquake, the shaking effect of the earthquake caused cleavages and lateral spreading deformations in the road embankment at the Çöçelli junction of the Gaziantep-Kahramanmaraş road (Figure 10). These surface deformations in anthropogenic ground structures do not have the characteristic of being close to the surface fracture of the fault. On the other hand, the intensity of the earthquake-induced shaking is decisive for such surface deformations. Two main

processes were influential in the occurrence of this earthquake-induced deformation. One of them is that the shaking force of the earthquake directly destabilizes the embankment, causing cleavages, lateral spreading, and sinking deformations. The other process is indirect impact. This intersection embankment was constructed on water-saturated, detrital, alluvial, and unconsolidated weak ground. Such grounds have a high risk of liquefaction, sinking, and collapse during earthquakes. In addition, these types of soils are poor conductors for earthquake waves. In such soils, seismic waves travel more slowly, and this causes more damage. The road embankment at the Çöçelli intersection was built on this type of ground. Therefore, due to the magnifying role of the ground on the shaking effect of the seismic waves, the cleavages, lateral spreading, and sinking deformations of the intersection embankment were more magnified.



Figure 10: Gaziantep-Kahramanmaraş road Çöçelli intersection, cleavages, lateral spreading, and sinking deformations in the intersection road embankment (Figure 2).

## 6. Conclusion

The surface fracture of the ±85 km long Pazarcık segment, which is a part of the sinistral strike-slip EAF formed by the February 06, 2023 earthquake, was followed, and the evaluations were made subsequently by investigating the geomorphological deformations in the field.

Compression ridges and transtensional depressions were formed on the surface fracture traced between Türkoğlu and Gölbaşı. The main reason for these morphological deformations is the curvilinear fracture of the sinistral strike-slip fault. The pressure ridge, one of the main morphological units in the study area consisting of the Kandil, Çataldağ, and Sakarkaya mountain peaks, is the morphological result of the curvilinearity of the Pazarcık fault. Compression ridges on the surface rupture, formed by the February 06, 2023 earthquake, developed in the alluvial plain NE of Sakarkaya pressure ridge. Opening depressions are other examples of the geomorphologic deformation caused by the last earthquake within the Türkoğlu depression.

Liquefaction structures classified into different types were observed on the alluvial plain near Sakarkaya in the SW part of the Gölbaşı depression. Liquefaction blowing, consisting of silt and fine sand, linearly arranged liquefaction eruptions, clustered samples, and spreading or flowing samples, were considered as different liquefaction structure examples.

Rock falls were observed on the surface rupture in the slopes of the Çataldağ-Sakarkaya pressure ridge. Discontinuities caused by previous tectonic activities on the rocks and deformations, the effect of physical weathering, have weakened the durability of the rock slopes. As a result, on February 06, 2023, earthquake rockfalls occurred on such slopes.

Ground slidings and lateral spreadings in the poor ground are also examples of geomorphological deformations caused by the shaking effect of the February 06, 2023 earthquake. Typical sliding, cleavage, and sinking samples were observed on the southern shores of Gölbaşı Lake. The sampled sliding, cleavage, and sinking deformations were realized as the movement of the unconsolidated, slightly sloping embankment towards Gölbaşı Lake in the slope direction due to the shaking effect of the earthquake. A typical example of lateral spreading in the field is the spreading deformation in the road embankment at the Çöçelli junction of the Gaziantep-Kahramanmaraş road. In this lateral spreading example, the road and intersection embankment lost its stability due to the shaking effect of the earthquake and was deformed by cleavages, lateral spreading, and sinking.

### Conflict of Interest:

The authors declared no conflict of interest.

### Author contribution:

The planning, scientific content, and design of the study were done by H.T. Fieldwork (surveying and UAV data collection, photography), and preparation of maps was carried out by H.T. and O.S. Data description, explanation, and writing of the manuscript was realized by H.T.

## References

- AFAD (2023). *06 Şubat 2023 Kahramanmaraş (Pazarcık ve Elbistan) Depremleri Saha Çalışmaları Ön Değerlendirme Raporu*. [https://deprem.afad.gov.tr/assets/pdf/Arazi\\_Onrapor\\_28022\\_023\\_surum1\\_revize.pdf](https://deprem.afad.gov.tr/assets/pdf/Arazi_Onrapor_28022_023_surum1_revize.pdf)
- Aktif Tektonik Araştırma Grubu (ATAG). (2023). *Yer bilimlari veri kataloğu*. <https://atag.itu.edu.tr/v4/?p=135>
- Armijo, R., Meyer, B., Hubert, A., & Barka, A. (1999). Westward propagation of the North Anatolian fault into the northern Aegean: Timing and kinematics. *Geology*, 27(3), 267-270. [https://doi.org/10.1130/0091-7613\(1999\)027<0267:WPOTNA>2.3.CO;2](https://doi.org/10.1130/0091-7613(1999)027<0267:WPOTNA>2.3.CO;2)
- Aydan, Ö. (2016). Large Rock Slope Failures Induced by Recent Earthquakes. *Rock Mechanics and Rock Engineering*, 49, 2503–2524. <https://doi.org/10.1007/s00603-016-0975-3>
- BDTİM (2023). Boğaziçi Üniversitesi Kandilli Rasathanesi ve Deprem Araştırma Enstitüsü Bölgesel Deprem-Tsunami İzleme ve Değerlendirme Merkezi. <http://www.koeri.boun.edu.tr/sismo/2/tr/>
- Burbank, D.W. & Anderson, R.S. (2008). *Tectonic geomorphology*. Blackwell Science Ltd. ISBN 978-0-632-04386-6.
- Chen, X-li., Liu, C-guo., Wang, M-ming. & Zhou, Q. (2018). Causes of unusual distribution of coseismic landslides triggered by the Mw 6.1 2014 Ludian, Yunnan, China earthquake. *Journal of Asian Earth Sciences*, 159, 17-23. <https://doi.org/10.1016/j.jseaes.2018.03.010>
- Christie-Blick, N, & Biddle, K. T. (1985). Deformation and basin formation along strike-slip faults. In K. T. Biddle & N. Christie-Blick (Eds.), *Strike-slip deformation, basin formation and sedimentation*. Society of Economic Paleontologists and Mineralogists Special Publication, 37, 1–34. Doi:[10.2110/pec.85.37.0001](https://doi.org/10.2110/pec.85.37.0001)
- Cunningham, W.D. & Mann, P. (2007). Tectonics of strike-slip restraining and releasing bends. İçinde: Cunningham, W. D. & Mann, P. (eds) *Tectonics of Strike-Slip Restraining and Releasing Bends*. Geological Society, London, Special Publications, 290, 1–12. <https://www.lyellcollection.org/doi/10.1144/SP290.1>
- Dewey, J.F., Hempton, M.R., Kidd, W.S.F., Şaroğlu, F. & Şengör, A.M.C., (1986). Shortening of continental lithosphere: the neotectonics of Eastern Anatolia—a young collision zone, *Geological Society Special Publication*, 19(1), 1–36.
- Dewey, J.E., Holdsworth, R.E. & Strachan, R.A. (1998). Transpression and transtension zones. In: Holdsworth, R.E., Strachan, R.A., Dewey, J. E (eds) 1998. *Continental Transpressional and Transtensional Tectonics*. Geological Society, London, Special Publications, 135, 1-14. <https://www.lyellcollection.org/doi/pdf/10.1144/gsl.sp.1998.135.01.01>
- Eitzenberger, A. (2012). *Wave Propagation in Rock and the Influence of Discontinuities*. Doctorial Thesis, Division of Mining and Geotechnical Engineering, Department of Civil, Environmental and Natural Resources Engineering, Luleå University of Technology, SE-971 87 Luleå, SWEDEN. <https://www.diva-portal.org/smash/get/diva2:990707/FULLTEXT01.pdf>

- Güvercin, S.E., Karabulut, H., Konca, A.Ö., Doğan, U. & Ergintav, S. (2022). Active seismotectonics of the East Anatolian Fault. *Geophysical Journal International*, 230, 50–69. <https://doi.org/10.1093/gji/ggac045>
- Hack, R., Alkema, D., Kruse, G.A.M., Leenders, N. & Luzi, L. (2007). Influence of earthquakes on the stability of slopes. *Engineering Geology*, 91(1), 4–15. <https://doi.org/10.1016/j.enggeo.2006.12.016>
- Hempton, M.R. (1987). Constraints on Arabian Plate motion and extensional history of the Red Sea. *Tectonics*, 6, 687–705.
- Huang, L. & Liu, C.-y. (2017). Three types of flower structures in a divergent-wrench fault zone. *Journal of Geophysical Research: Solid Earth*, 122, 10478–10497. <https://doi.org/10.1002/2017JB014675>
- Karabacak, V., Özkaymak, Ç., Sözbilir, H., Tatar, O., Aktuğ, B., Özdağ, Ö.C., Çakır, R., Aksoy, E., Koçbulut, F., Softa, M., Akgün, E., Demir, A. & Arslan, G. (2023). The 2023 Pazarlık (Kahramanmaraş, Türkiye) Earthquake (Mw: 7.7): Implications for surface rupture dynamics along the East Anatolian Fault Zone. *Journal of the Geological Society*, 180 (3) <https://doi.org/10.1144/jgs2023-020>
- Khalifa, A., Çakır, Z., Owen, L.A. & Kaya, Ş. (2018). Morphotectonic analysis of the East Anatolian Fault, Turkey. *Turkish Journal of Earth Sciences*, 27, 110-126. doi:10.3906/yer-1707-16
- KRDAE (2023). B.Ü. 06 Şubat 2023 Ekinözü Kahramanmaraş Depremi Basın Bülteni. Kandilli Rasathanesi ve DAE, Bölgesel Deprem-Tsunami İzleme Ve Değerlendirme Merkezi. [http://www.koeri.boun.edu.tr/sismo/2/wp-content/uploads/2023/02/20230206\\_1024\\_KAHRAMANMA\\_RAS.pdf](http://www.koeri.boun.edu.tr/sismo/2/wp-content/uploads/2023/02/20230206_1024_KAHRAMANMA_RAS.pdf)
- Kürçer, A., Elmacı, H., Özdemir, E., Güven, C., Güler, T., Avcu, İ. & Özalp, S. (2023a). 06 Şubat 2023 Pazarlık (Kahramanmaraş) Depremi (Mw 7,7) Saha Gözlem Raporları Serisi 1- Amanos Segmenti. [https://www.mta.gov.tr/files/img/popup/06022023\\_pazarcik%4B1k\\_depremi\\_saha\\_gozlem\\_raporu\\_1\\_amanos\\_segm\\_enti.pdf](https://www.mta.gov.tr/files/img/popup/06022023_pazarcik%4B1k_depremi_saha_gozlem_raporu_1_amanos_segm_enti.pdf)
- Kürçer, A., Elmacı, H., Özdemir, E., Güven, C. & Özalp, S. (2023b). 06 Şubat 2023 Kahramanmaraş Depremleri Genişletilmiş Bilgi Notu. MTA Genel Müdürlüğü, Jeoloji Etütleri Dairesi Başkanlığı. [https://www.mta.gov.tr/v3.0/sayfalar/bilgi-merkezi/deprem/pdf/Genisletilmis\\_Bilgi\\_Notu\\_06\\_Subat\\_2023%20KMaras\\_Depremleri.pdf](https://www.mta.gov.tr/v3.0/sayfalar/bilgi-merkezi/deprem/pdf/Genisletilmis_Bilgi_Notu_06_Subat_2023%20KMaras_Depremleri.pdf)
- Maden Tetik Arama (2023). *Yer bilimleri harita görüntüleyici*. Maden Tetik Arama ve Genel Müdürlüğü. <http://yerbilimleri.mta.gov.tr/anasayfa.aspx>
- Massey, C. I., Olsen, M. J., Wartman, J., Senogles, A., Lukovic, B., Leshchinsky, B. A., Archibald, G., Litchfield, N., Van Dissen, R., de Vilder, S. & Holden, C. (2022). Rockfall Activity Rates Before, During and After the 2010/2011 Canterbury Earthquake Sequence. *Journal of Geophysical Research: Earth Surface*, 127(3): e2021JF006400. <https://doi.org/10.1029/2021JF006400>
- McClay, K. & Bonora, M. (2001). Analog models of restraining stepovers in strike-slip fault systems. *AAPG Bulletin*, 85(2), 233–260. [http://activetectonics.asu.edu/ActiveFaultingSeminar/Papers/McClay\\_Bonora\\_2001.pdf](http://activetectonics.asu.edu/ActiveFaultingSeminar/Papers/McClay_Bonora_2001.pdf)
- Moore, J.R., Gischig, V., Amann, F., Hunziker, M., Hunziker, M. & Burjanek, J. (2012). Earthquake-triggered rock slope failures: Damage and site effects. *Conference: Proceedings 11th International & 2nd North American Symposium on Landslides*. [https://www.researchgate.net/publication/260981734\\_Earthquake-triggered\\_rock\\_slope\\_failures\\_Damage\\_and\\_site\\_effects](https://www.researchgate.net/publication/260981734_Earthquake-triggered_rock_slope_failures_Damage_and_site_effects)
- NRC (1985). *Liquefaction of soil during earthquakes*. PB86-163110 Final Report. National Research Council, Commission on Engineering and Technical System. National Science Foundation, National Academy Press, Washington. <https://nehrpsearch.nist.gov/static/files/NSF/PB86163110.pdf>
- Rauch, A.F. (1997). *Soil liquefaction in earthquakes* 2.1. Definition of Soil Liquefaction Chapter 2, 7-18. <https://vtechworks.lib.vt.edu/bitstream/handle/10919/30346/Chp02.pdf?sequence=7>
- Roy, N. & Sarkar, R. (2015). Effect of mechanical properties of discontinuity on the seismic stability of tunnel in jointed rock mass. *50th Indian Geotechnical Conference 17th – 19th December 2015, Pune, Maharashtra, India*. [https://www.researchgate.net/publication/287330896\\_EFFECT\\_OF\\_MECHANICAL\\_PROPERTIES\\_OF\\_DISCONTINUITY\\_ON\\_THE\\_SEISMIC\\_STABILITY\\_OF\\_TUNNEL\\_IN\\_JOINTED\\_ROCK\\_MASS](https://www.researchgate.net/publication/287330896_EFFECT_OF_MECHANICAL_PROPERTIES_OF_DISCONTINUITY_ON_THE_SEISMIC_STABILITY_OF_TUNNEL_IN_JOINTED_ROCK_MASS)
- Sciarra, A., Cantucci, B., Buttinelli, M., Galli, G., Nazzari, M., Pizzino, L. & Quattrocchi, L. (2012). Soil-gas survey of liquefaction and collapsed caves during the Emilia seismic sequence. *Annals of Geophysics*, 55(4), 803-809. doi: 10.4401/ag-6122. <https://www.annalsofgeophysics.eu/index.php/annals/article/view/6122>
- SBB (2023). *2023 Kahramanmaraş ve Hatay Depremleri Raporu*. Türkiye Cumhuriyeti Cumhurbaşkanlığı Strateji ve Bütçe Başkanlığı. <https://www.sbb.gov.tr/wp-content/uploads/2023/03/2023-Kahramanmaraş-ve-Hatay-Depremleri-Raporu.pdf>
- Shao, Z-Fu, Zhong, J-Hua, Howell, J., Hao, B., Luan, X-Wu, Liu, Z-Xuan, Ran, W-Min, Zhang, Y-Feng, Yuan, H-Qi, Liu, J-Jing, Ni, L-Tian, Song, G-Xian, Liu, J-Lin, Zhang, W-Xin. & Zhao, B. (2020). Liquefaction structures induced by the M5.7 earthquake on May 28, 2018 in Songyuan, Jilin Province, NE China and research implication. *Journal of Palaeogeography*, 9, 3. <https://doi.org/10.1186/s42501-019-0053-3>
- Singeisen, C., Massey, C., Wolter, A., Kellett, R., Bloom, C., Stahl, T., Gasston, C. & Jones, K. (2022). Mechanisms of rock slope failures triggered by the 2016 Mw 7.8 Kaikōura earthquake and implications for landslide susceptibility. *Geomorphology*, 415, 108386. <https://doi.org/10.1016/j.geomorph.2022.108386>
- Sylvester, A.G. (1988). Strike-Slip Faults. *Geological Society of America Bulletin*, 100(11), 1666-1703. DOI:10.1130/0016-7606(1988)100<1666:ssf>2.3.co;2
- Şengör, A.M.C. & Yılmaz, Y. (1981). Tethyan evolution of Turkey: A plate tectonic approach. *Tectonophysics*, 75, 181–241.
- Tang, H., Wu, Z., Che, A., Yuan, C. & Deng, Q. (2012). Failure Mechanism of Rock Slopes under Different Seismic Excitation. *Hindawi, Advances in Materials Science and Engineering*, 2021, Article ID 8866119, 16 pages. <https://doi.org/10.1155/2021/8866119>

- Turođlu, H. & Sarıgöl, O. (2023, March 27). *DAF Pazarcık segmenti, 06 Şubat 2023 depremi jeomorfolojik deformasyon örnekleri* [Video]. YouTube.  
<https://www.youtube.com/watch?v=JvGLSwJ5J6U&t=357s>
- Tuttle, M.P., Hartleb, R., Wolf, L. & Mayne, P.W. (2019). Paleoliquefaction Studies and the Evaluation of Seismic Hazard. *Geosciences*, 9(7), 311.  
<https://doi.org/10.3390/geosciences9070311>
- Utkucu, M., Uzunca, F., Durmuş, H., Nalbant, S., Sert, S. (2023). The 2023 Pazarcık (Mw=7.8) And Elbistan (Mw=7.6), Kahramanmaraş Earthquakes in The Southeast Türkiye. Sakarya University, Disaster Management Application and Research Center and Department of Geophysic.  
<http://www.aym.sakarya.edu.tr/2023/02/24/the-2023-pazarcik-mw7-8-and-elbistan-mw7-6-kahramanmaras-earthquakes-in-the-southeast-turkiye/>
- Vallejo, L.E. (1992). Liquefaction zones predicted by the type of stresses induced by the ends of fault segments. *Earthquake Engineering, Tenth World Conference-1992, Balkema, Rotterdam*, ISBN 9054100605, 1355-1359.  
[https://www.iitk.ac.in/nicee/wcee/article/10\\_vol3\\_1355.pdf](https://www.iitk.ac.in/nicee/wcee/article/10_vol3_1355.pdf)
- Yılmaz, Y. (1993). New evidence and model on the evolution of the southeast Anatolian orogen, *Bulletin of the Geological Society of America*, 105, 251–271.
- Zheng, L., Wu, Y., Zhu, Y., Ren, K., Wei, Q., Wu, W. & Zhang, H. (2022). Investigating the Role of Earthquakes on the Stability of Dangerous Rock Masses and Rockfall Dynamics. *Frontiers in Earth Science*, 9, 824889.  
<https://doi.org/10.3389/feart.2021.8248>